

Palaeogene–Neogene sedimentary and tectonic evolution of the Yinchuan Basin, western North China Craton

Xiao-Bo Liu, Jian-Min Hu, Wei Shi, Hong Chen & Ji-Yuan Yan

To cite this article: Xiao-Bo Liu, Jian-Min Hu, Wei Shi, Hong Chen & Ji-Yuan Yan (2019): Palaeogene–Neogene sedimentary and tectonic evolution of the Yinchuan Basin, western North China Craton, International Geology Review, DOI: [10.1080/00206814.2019.1591309](https://doi.org/10.1080/00206814.2019.1591309)

To link to this article: <https://doi.org/10.1080/00206814.2019.1591309>

 View supplementary material 

 Published online: 21 Mar 2019.

 Submit your article to this journal 

 View Crossmark data 

ARTICLE



Palaeogene–Neogene sedimentary and tectonic evolution of the Yinchuan Basin, western North China Craton

Xiao-Bo Liu^a, Jian-Min Hu^a, Wei Shi^{a,b}, Hong Chen^a and Ji-Yuan Yan^a

^aInstitute of Geomechanics, Chinese Academy of Geological Sciences, Beijing, China; ^bKey Laboratory of Neotectonic Movement and Geohazard, Ministry of Natural Resources, Beijing, China

ABSTRACT

The Yinchuan Basin is one of the Cenozoic rift basins around the Ordos Block in the North China Craton and is also the frontier zone of the north-eastern expansion of the Tibetan Plateau. Due to its special geotectonic position, the views on formation mechanisms and evolution process of the Yinchuan Basin are still controversial. Herein, we present a detailed study of the Palaeogene–Neogene sediment sequence in and around the basin coupled with activities of faults. Our results demonstrate that the Yinchuan Basin mainly underwent two evolutionary stages during the Palaeogene–Neogene. At the first stage, from the Eocene to the late middle Miocene, the Yinchuan Basin was dominated by a NW–SE extension with deposits of the Sikouzi, Qingshuiying, and Zhanganbu Formations. The incipient Yinchuan Basin was developed on pre-existing basement faults and deposits of the Sikouzi Formation (E_2s). The Qingshuiying Formation (E_3q) consists mainly of lacustrine mudstones with unified eastward palaeocurrents in the basin and its periphery, indicating that a unitive lake existed in the studied area during the Oligocene. The alluvial fan conglomerates in the lower part of the Zhanganbu Formation (N_{1z}) developed on both sides of the Helan Mountains as a response to the initial uplift of the mountains. At the second stage, from the late Miocene to the Pliocene, the sedimentation of the Yinchuan Basin was dominantly controlled by a NE–SW compression that led to a brief uplift of the study area. After a short sedimentary discontinuity, the Ganhegou Formation (N_{1-2g}) was deposited in the basin. The evolutionary features of the two stages of the basin are consistent with that of the regional tectonics. It is suggested that the tectonic evolution of the Yinchuan Basin in the early and late stages was mainly controlled by the Pacific plate's subduction and the northeastward expansion of the Tibetan Plateau, respectively.

ARTICLE HISTORY

Received 12 November 2018
Accepted 3 March 2019

KEYWORDS

Yinchuan Basin; Tectonic evolution; Tibetan Plateau; Helan Mountains; Palaeogene–Neogene

1. Introduction

The complex interactions of plate boundary forces result in multistage evolution and deformation in the East Asian continent, including complex basin-mountain architecture and evolution (Li *et al.* 2013; 2017b). These features have been correlated to the Mesozoic–Cenozoic convergence between the Pacific and Eurasian plates (Ren *et al.* 2002; Liu *et al.* 2007; Qi and Yang 2010; Li *et al.* 2013; Kim *et al.* 2015; Qiu *et al.* 2015), Cenozoic convergence between the Indian and Eurasian plates (Molnar and Tapponnier 1975; Philippe and Jose 1984; Harrison *et al.* 1992; Pan 1999; Yin and Harrison 2000; An *et al.* 2001; Tapponnier *et al.* 2001). For example, multiple geological investigations have proposed that the Mesozoic–Cenozoic structural deformation, rifting and destruction of the North China Craton (NCC) were related to the far-field effects of the western Pacific plate's subduction (Wu *et al.* 2005;

Menzies *et al.* 2007; Zheng *et al.* 2009; Liu *et al.* 2017b). The Yinchuan Basin is one of the Cenozoic rift basins around Ordos sub-block and has always been part of the NCC. Therefore, its formation and evolution should be closely related to the evolution of the NCC. In addition, the uplift of the Tibetan Plateau response to the Indian plate's subduction is one of the most important factors affecting the tectonic evolution of the east Asian continent since the Cenozoic. Its far-field effects are obvious as they led to the environmental changes (Quade 1989; An *et al.* 2006; Molnar *et al.* 2010; Li 2013; Li *et al.* 2014, 2017; Peng *et al.* 2016) and the formation of a unique basin-mountain architecture on the periphery of the plateau, including the arc-shaped tectonic belt in the north-eastern margin of the Tibetan Plateau (Burchfiel *et al.* 1991; Wang *et al.* 2013; Shi *et al.* 2015). The Yinchuan Basin directly connects with the arc-shaped tectonic belt. Therefore, it may be an

important part of the deformation zone of the Tibetan Plateau and a new forefront of the north-eastern expansion of the Tibetan Plateau.

Due to its special geotectonic position, there has been a scientific controversy over the formation and tectonic evolution of the Yinchuan Basin. The first hypothesis suggests that the basin is comparable to an 'Impactogen' (Burke 1980; Hancock and Bevan 1987) and it formed as a result of north-east compression during the collision between the Indian and Eurasian plates (Molnar and Tapponnier 1975; Tapponnier *et al.* 1982; Zhang *et al.* 1990, 1998, 1999b; Deng *et al.* 1999; Chen *et al.* 2004). The second hypothesis considers the Yinchuan Basin as a rift basin in the NCC, which formed in an extensional regime (Uyeda and Kanamori 1979; Tian *et al.* 1992; Ren *et al.* 2002; Zhang *et al.* 2006; Lei 2016). This NW–SE extensional regime is related to the back-arc expansion driven by the subduction of the Pacific plate beneath the Eurasian plate (Tian *et al.* 1992; Northrup *et al.* 1995; Ren *et al.* 2002; Zhang *et al.* 2006). The third hypothesis suggests that the Yinchuan Basin is an active rift basin that originated from crustal extension driven by upward arching of the upper mantle beneath the basin (Li *et al.* 1999; Deng *et al.* 2006; Wang and Li 2008; Huang *et al.* 2016).

Therefore, two questions arise: (1) What are the evolutionary processes of the basin and its evolutionary mechanism? (2) When did the far field effect of the NE expansion of the Tibetan Plateau spread to the Yinchuan Basin? To address these questions, we present a detailed study of the Palaeogene–Neogene sedimentary processes in the basin based on data from the boreholes in the basin and from investigations on several geological sections. The activities of faults in and around the basin are also analysed to best understand the tectonic setting of the basin. The magnetochronology data of the XL15-1-01 borehole of the south part of the Yinchuan Basin coupled with previous biostratigraphy results constrain the ages of the sedimentary units and the tectonic events. Finally, we provide a model of the tectonic evolution of the Yinchuan Basin and discuss the possible controlling mechanisms for the individual stages.

2. Geological setting

The NNE–SSW-oriented Yinchuan Basin is adjacent to the Alax sub-block on the west side, the Ordos sub-block on the east side, and the arc-shaped tectonic belt on the northeast margin of the Tibetan Plateau on the south side (Figure 1(a)). The Yinchuan Basin is also one of the Cenozoic rift basins around the Ordos Block (Figure 1(b)).

The Basin is >180 km long and 42–60 km wide and is crossed by the Yellow River. The Helan Mountain, Niushou Mountain and Zhuozi Mountain form the western, southern and northern boundary of the basin (Figure 2(a)), respectively, where the pre-Cenozoic rocks are mainly exposed. The Upper Ordovician, Silurian, Devonian, lower Carboniferous and Upper Cretaceous strata were missing from the Yinchuan Basin and its periphery. The Precambrian rocks composed mainly of gneiss, quartzite schist and slate. The Cambrian strata consist mainly of limestone. The Ordovician strata are limestone interbedded with sandstone and shale. The middle-upper Carboniferous strata composed mainly of sandstone shale, limestone and coal seams. The lower Permian strata consist of grey–green sandy shale interbedded with sandstone, and the upper Permian is a red rock series composed of sandstone and mudstone. The Triassic strata are mainly feldspar quartz sandstone, lithic feldspathic sandstone, feldspar sandstone and a small amount of purple–red silty mudstone. The Lower Jurassic strata are grey sandstone interbedded with black shale and coal seam. The Middle Jurassic strata are yellow–green, grey–white sandstone interbedded with grey mudstone. The Upper Jurassic strata consist mainly of purple–red sandstone and conglomerate, interbedded with thin layer of shale and thin coal seams. The Lower Cretaceous strata are mainly brick-red conglomerate. The basement strata of the Yinchuan Basin are composed of Palaeozoic strata and pre-Palaeozoic strata, and there may be Jurassic and Cretaceous strata in the south.

The Yinchuan Basin has accumulated an approximately 6000 m and 1600 m thick layer of Palaeogene–Neogene and Quaternary sediments, respectively, reflecting the long-term extension in the region (Deng *et al.* 2006; Feng *et al.* 2011; Lin *et al.* 2015). The Palaeogene–Neogene sediments in the basin are divided into the Sikouzi, Qingshuiying, Zhangenbu, and Ganhegou Formations from the oldest to the youngest. It should be noted that the Hongliugou Formation was renamed as the Zhangenbu Formation by Ningxia Bureau of Geology and Mineral Resources (2017). This Formation is mainly exposed in the Qingtongxia area and western Ganchengzi village to the southwest of the Yinchuan Basin and in the east and west sides of the Helan Mountains.

The Yinchuan Basin is bounded by the Helan Mountains Piedmont fault (HLPF) on the west side, the Huanghe (Yellow River) fault (HHF) on the east side, the Zhengyiguan fault (ZYGf) on the north side, and the Liumugao–Niushoushan fault (LMG–NSF) on the south side (Figure 2(a)). In addition, two unexposed faults are observed in reflection seismic profiles (Figure 2(b)):

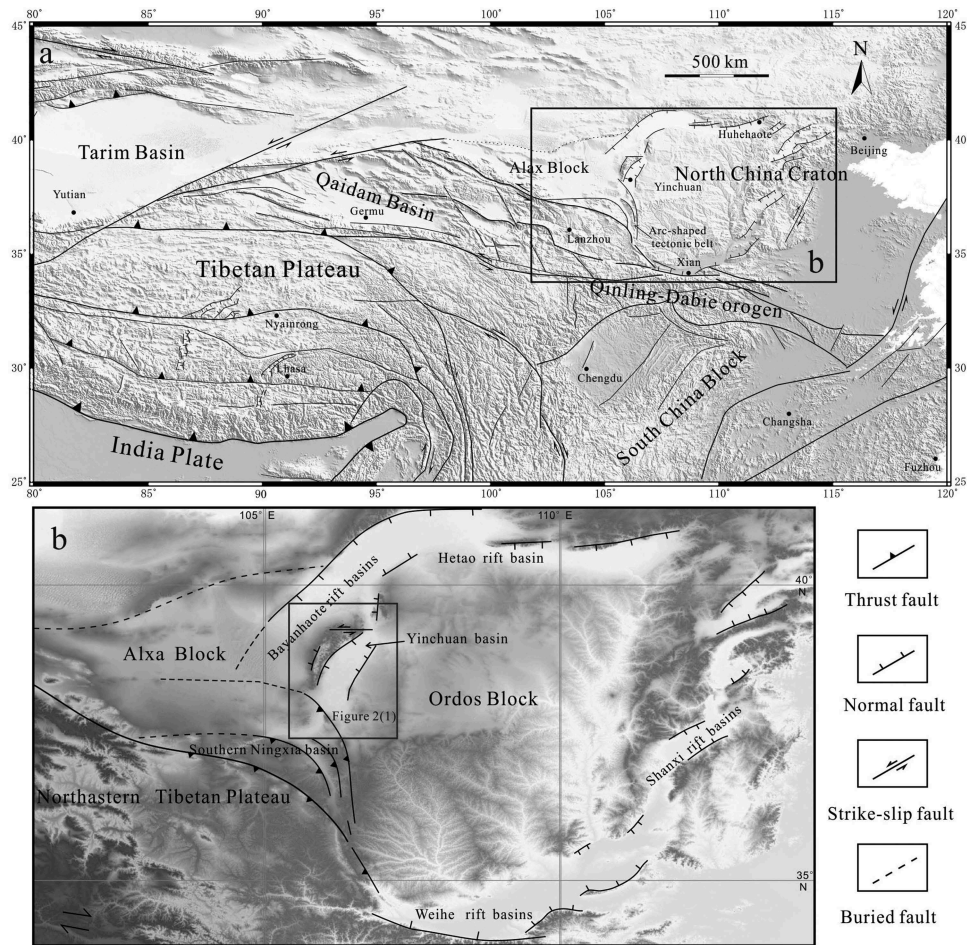


Figure 1. (a) Schematic tectonic map of the Tibetan Plateau and adjacent areas (modified from Shi *et al.* (2015)). (b) General tectonic setting of the western North China Craton showing the location of similar basins around the Yinchuan Basin.

the Luhutai fault and the Yinchuan–Pingluo fault (Chai *et al.* 2007; Fang *et al.* 2009; Feng *et al.* 2011; Huang *et al.* 2016; Liu *et al.* 2017a). Geological interpretations of seismic reflection profiles (Fang *et al.* 2009; Hou *et al.* 2014; Liu *et al.* 2017a) showed a stepped- or slope-like basement and a thick sedimentary fill in the central section of the basin that thins to the basin margins (Figure 2(b)).

3. Basin stratigraphy

3.1 Age of sedimentary units

In this study, the age of sedimentary units in the Yinchuan Basin was constrained by integrating available data of magnetostratigraphy and biostratigraphy. The Sikouzi Formation dates back to the Eocene (Ningxia Bureau of Geology and Mineral Resources 1996; Han *et al.* 2008). The Qingshuiying Formation dates back to the Oligocene (Sun 1982; Ningxia Bureau of Geology and Mineral Resources 1996). The results of the magnetostratigraphy study on the XL15-1-01 borehole (Figure 2(a)) in the SE Yinchuan Basin show that the upper age limit of the Qingshuiying

Formation is 21.32 Ma. The Zhangenbu Formation dates back to the early Miocene–late middle Miocene (21.32–10.17 Ma), and the Ganhegou Formation to the late Miocene–Pliocene (9.58–2.77 Ma) (Liu *et al.* 2019).

3.2 Sedimentary sequence and facies association

Herein, the Palaeogene–Neogene sediments of the Yinchuan Basin are divided into 21 lithofacies (Supplementary Table 1) according to the sediment colour, grain size, sedimentary structures, and the principle of sedimentary facies analysis (Miall 1977, 1978, 1996; Horton and Schmitt 1996; Song 2006; Saylor *et al.* 2011; Gobo *et al.* 2015). In addition, we identify six sedimentary environments according to their lithofacies combinations: lacustrine (L), delta (D), fan delta (FD), alluvial fan (AF), braided river (BR), and meandering river (MR) (Supplementary Table 2). A detailed classification of the Palaeogene–Neogene sedimentary sequence and their lithofacies is presented below.

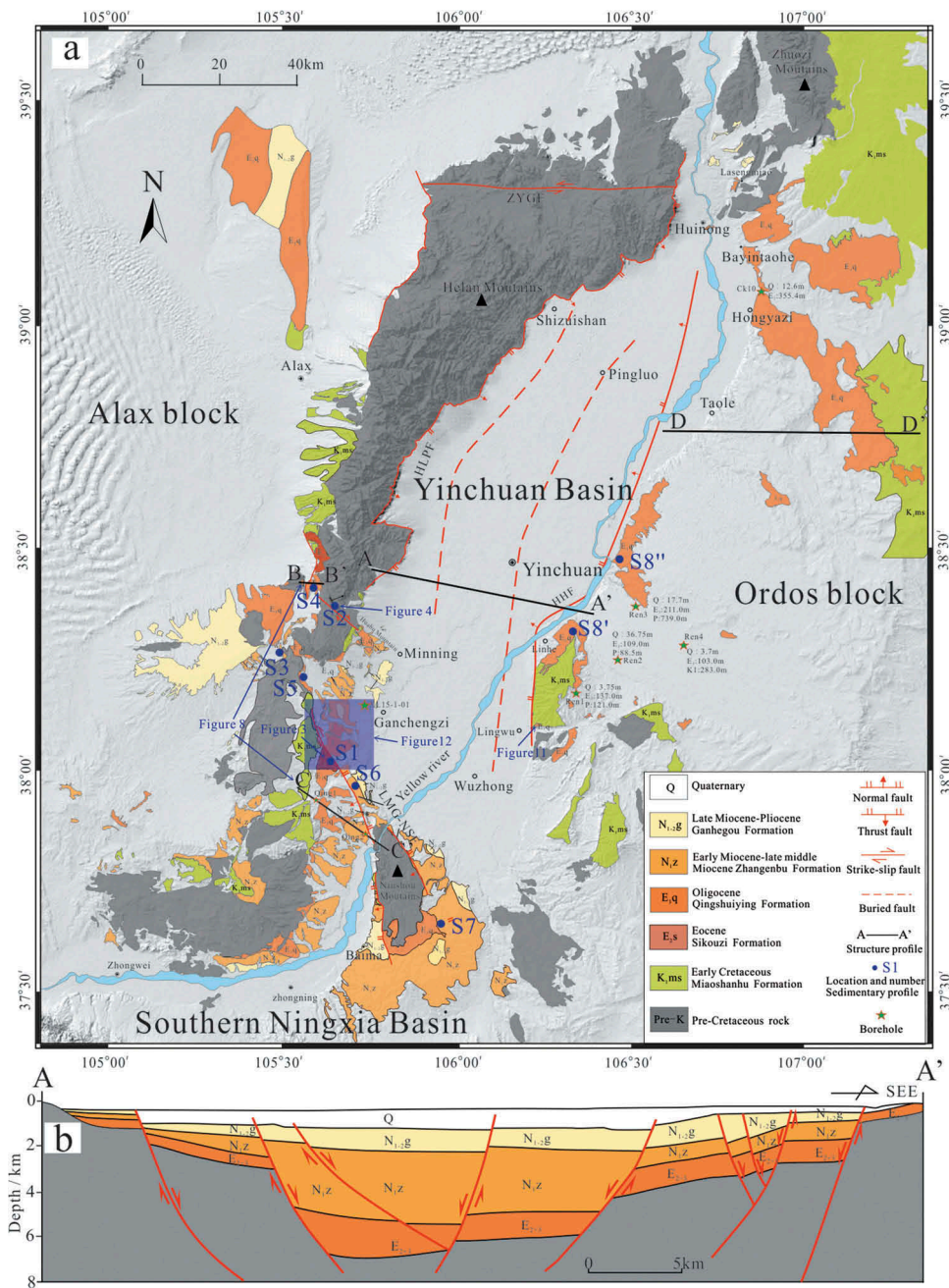


Figure 2. Simplified geological map (a) and the synthesized profile (b) to show the deep-basement structure of the Yinchuan Basin. (a) was modified after regional 1:200,000 geological maps of the Ningxia Hui Autonomous Region and Inner Mongolia Autonomous Region. (b) was modified after Fan *et al.* (2002), Fang *et al.* (2009), and Hou *et al.* (2014). Small letters mark the following stratigraphic profiles: Hongaodunshan (S1); inner Helan Mountains (S2); Emeishan (S3); Jijinzi (S4); Hongguozi (S5); northern Qingtongxia (S6); eastern Niushou Mountains (S7); and the eastern Yinchuan Basin (S8' and S8'').

HLPF – Helan Mountain piedmont fault, HHF – Huanghe (Yellow River) fault, ZYGF – Zhengyiguan fault, LMG-NSF – Liumugao-Niushoushan fault.

3.2.1 Sikouzi formation (E₂s)

The Sikouzi Formation represents the oldest Cenozoic strata within the Yinchuan Basin and rests unconformably on the Miaoshanhu Formation (K₁ms) or older strata. Sediments of the Sikouzi Formation are mainly exposed in the Hongaodunshan area of Qingtongxia County, on

the western margin of the Helan Mountain, and in the Helan Mountain (Figure 2(a)). The sediments of the Sikouzi Formation in the Yinchuan Basin, best represented by the ~320 m thick Hongaodunshan section (Figures 2(a)(S1) and 3), are subdivided into four units according to their lithofacies associations.

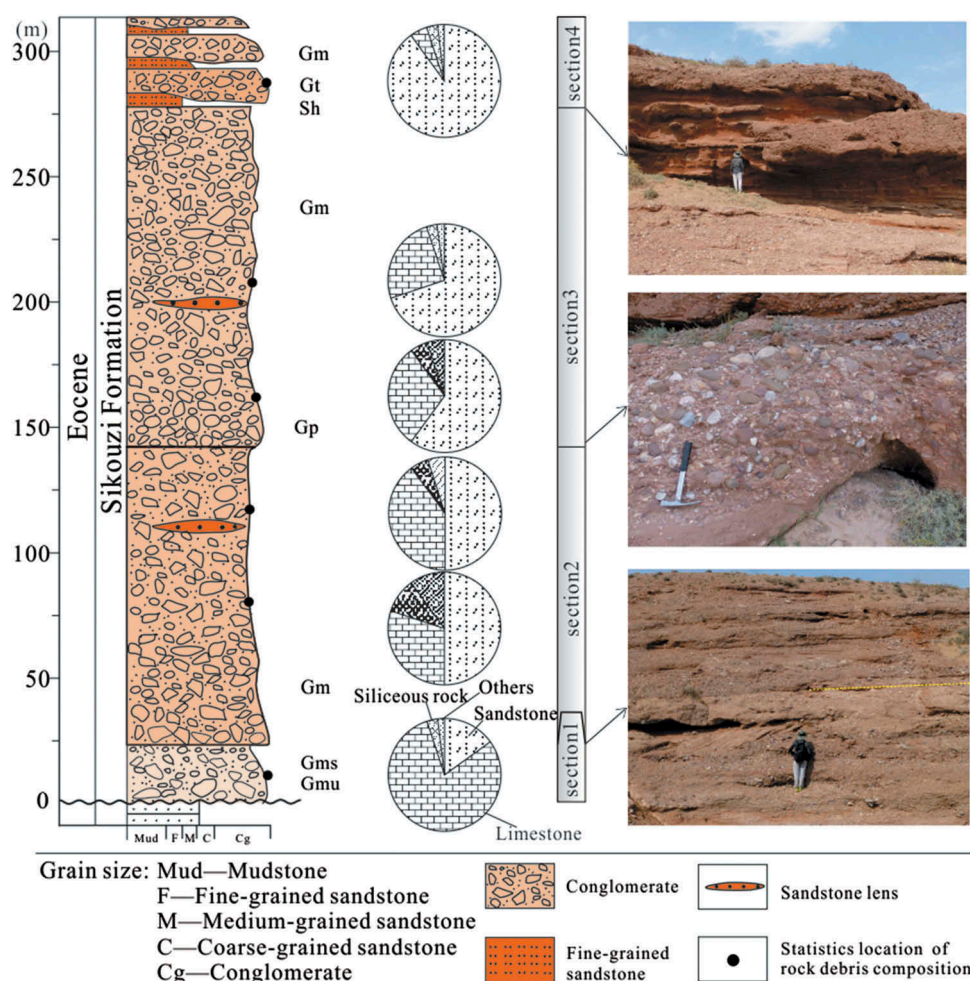


Figure 3. Stratigraphic log showing detritus composition, and representative field photographs of the Sikouzi Formation in the Hongaodunshan profile (See 'S1' on the Figure 2a(1) for location). Gm – Massive or crudely bedded gravel, Gms – Matrix-supported gravel, Gmu – poorly sorted granule–boulder conglomerate, Gt – stratified gravel with trough crossbeds, Gp – stratified gravel with planar crossbeds, Sh – very fine to very coarse sand with horizontal lamination.

The lowermost unit is mainly composed of a brown–red, thick-bedded conglomerate that contains sandstone lenses or beds (Figure 3). The conglomerate (facies Gms and Gmu) is matrix-supported and contains poorly sorted and sub-angular clasts of mainly limestone (75–80%), and grey–white quartz sandstone (~20%). These sediments are interpreted as AF deposits.

The lower–middle unit is dominated by a purple–red conglomerate (facies Gm) that also formed as an alluvial fan deposit. Compared with the lowermost part, the proportions of limestone (grey–black sandstone) gravels decrease (increase) to ~30% (~50%) (Figure 3). The abrupt change in gravel composition caused the darker colouration of the conglomerate compared with the lowermost part (Figure 3) and implies a different origin.

The middle–upper unit consists of a purple–red conglomerate. The imbricated, sub-rounded, and moderately sorted gravel clasts at the base of this part (Figure 3) are interpreted as debris flow deposits. In

the upper section, the gravels become sub-angular and poorly sorted and are composed mainly of purple–red sandstone (50%), greyish-green sandstone (~15%), limestone (~25%), and quartz (5%), as well as small amounts of other lithologies. The sedimentary environments are primarily debris flows and alluvial fans.

The uppermost part consists of a brick-red conglomerate with 0.5–2.0 m thick intervals of lenticular orange fine calcareous sandstone and siltstone (Figure 3; facies Sh). The sandstone shows cross-bedding. The moderately sorted gravels are mainly formed of purple–red sandstone (45–50%), greyish-green sandstone (35–40%), and limestone (~15%). These sediments are interpreted as fan-delta deposits.

In addition, the Sikouzi Formation, which forms the interior Helan Mountains on the western edge of the Yinchuan Basin (Figures 2(a)(S2) and 4), contains conglomerates interbedded with sandstones and sandy

mudstones that were deposited in an alluvial fan or a fan delta in a small catchment basin.

3.2.2 Qingshuiying formation (E_3q)

The Qingshuiying Formation composed mainly of fine clastic sediments dominated by mudstone and is widely distributed in the Yinchuan Basin and adjacent areas, where it rests conformably on the Sikouzi Formation. The sedimentary sequence of the Formation is best shown in the Jijingzi section on the western margin of the Helan Mountains (Figure 5(S4)), in the Hongguozi section on the western margin of the Yinchuan Basin (Figure 5(S5)), on the eastern margin section of the Yinchuan Basin (Figure 5(S8)), and in the XL15-1-01 borehole in the southwest part of Yinchuan Basin (Figure 5). The Qingshuiying Formation is subdivided into three units as follows.

The lower unit contains mainly purple–red conglomerates (facies Gms and Gmu; Supplementary Table 1) that are widely distributed in the Yinchuan Basin and in the western Helan Mountain. On the eastern margin of the Yinchuan Basin, the conglomerate (Figure 6(a); facies Gms) at the base of the Qingshuiying Formation is matrix-supported and poorly sorted. The clasts are mainly made of limestone and quartzite, 50–55% and ~40%, respectively. We interpret this portion of the Qingshuiying Formation as an alluvial fan deposit. In the upper section, the 20 m thick conglomerate shows a transition of rhythmic layers of orange–red conglomerate (facies Gmu) and orange–red mudstone (facies Mm). The grain-supported gravel is moderately sorted. The clasts are mainly made of limestone (~90%), and subordinate purple–red sandstone (6%). The sediments in the lower part of the Qingshuiying Formation on the western margin of the Helan Mountains (Figure 5(S4)) are similar to those occurring in the Yinchuan Basin. The 17 m thick lowermost part comprises medium- to fine-grained conglomerates containing purple–red sandstone, limestone, grey–green sandstone, and milky vein of quartz, at 50–55%, ~20%,

10–15%, and ~5%, respectively. In the upper section, the thick conglomerate layers show a transition of conglomerate layers interbedded with thin brown–red fine sandstone (facies Fm). The sediments in this lower part of the Qingshuiying Formation are interpreted as alluvial fan to fan-delta deposits.

The middle unit of the Qingshuiying Formation consists of sandstone and mudstone interbedded with gypsum. In the western margin of the Yinchuan Basin (Figure 5(S5)), the middle part of the Qingshuiying Formation is a thick layer of orange and red fine- to very fine-grained sandstone (facies Sd and Fm) with well-developed large-scale cross-bedding. This is interpreted as a delta deposit. In the Ganchengzi area of the SW Yinchuan Basin (XL15-1-01 borehole), the middle part of the Qingshuiying Formation consists of fine sandstone, siltstone, argillaceous siltstone, mudstone, and gypsum. The main body of the sequence is a massive brick-red mudstone (facies Fm and Fl) that shows traces of horizontal bedding. The mudstone is interbedded with thin layers of fibrous and laminated gypsum (facies Gy). Small- to medium-scale cross-bedding and wavy bedding characterize the fine-grained sandstone (facies St and Sp), showing no evidence of subaerial exposure. These lithological and sedimentary features suggest that the middle part of the Qingshuiying Formation in the Ganchenzi area was deposited in a shallow salt lake or delta environments. Stratigraphically equivalent strata on the eastern margin of the Yinchuan Basin consist of interlayered mudstone and argillaceous siltstone; however, no gypsum is present (Figure 6(b)). On the western margin of the Helan Mountain, the middle part of the Qingshuiying Formation consists of purple–red mudstone with horizontal bedding that is thinner than that in the Yinchuan Basin; these sediments are interpreted as lacustrine deposits.

The upper unit of the Qingshuiying Formation is widely distributed in the Yinchuan Basin and is

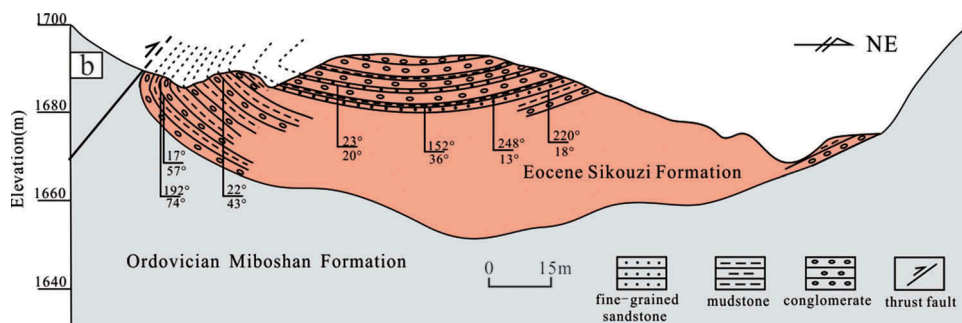


Figure 4. Stratigraphic profile of the Sikouzi Formation in the Helan Mountains (See 'S2' on the Figure 2a for location).

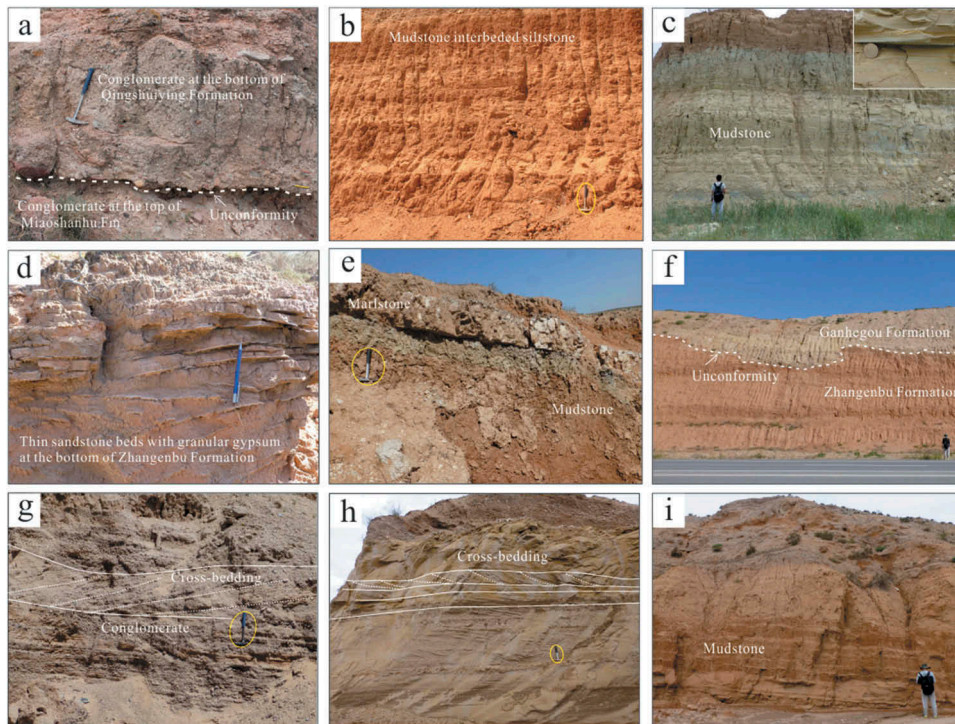


Figure 6. Field photographs of the Qingshuiying Formation from profile S8 (a–c), the Zhanganbu Formation from profile S7 (d–f), and the Ganhegou Formation from profile S6 (g–i) in the Yinchuan Basin.

siltstone (facies Sh and Fm) with horizontal stratification and the mudstone (facies Ml) with parallel bedding were likely deposited in a delta environment. The lower–middle unit of the Zhanganbu Formation consists of 20–30 m thick rhythmic siltstone (facies Sh) with horizontal bedding and massive mudstone (facies Fm and Mm). We interpret these sediments as lacustrine deposits.

The middle–upper unit of the Zhanganbu Formation, observed in the XL15-1-01 borehole and in the northern Qingtongxia area, consists of thick upward-fining rhythmic layers of fine conglomerate (facies Gm), sandstone (facies St and Fm), and mudstone (facies Mm). Each rhythmic layer begins with a 0.3–1.0 m thick conglomerate and thinly bedded medium- to coarse-grained quartz sandstone (facies St) covered by fine-grained sandstone, siltstone, and mudstone (facies Fm). Cross-bedding is developed in the medium- to coarse-grained quartz sandstone, whereas the mudstone shows horizontal bedding. A 2.0–5.0 m thick single conglomerate is present in the northern Qingtongxia area (Figure 5(S6)). Sediments in this middle–upper part of the Zhanganbu Formation are interpreted as meandering river deposits.

The uppermost unit of the Zhanganbu Formation is mainly composed of a 20–30 m thick layer of orange–red mudstone (Figure 6(f); facies Mm and Fm) with horizontal bedding. The mudstone was deposited in a lacustrine environment.

3.2.4 Ganhegou formation (N_{1-2g})

The Ganhegou Formation is composed of grey glauconite, grey–white quartz sandstone, orange–red siltstone, and silty mudstone that were deposited on the Zhanganbu Formation across a parallel and locally angular unconformity (Figure 6(f)). The Ganhegou Formation is mainly exposed on the eastern and western margins of the Niushou Mountain and has a more restricted areal distribution than the underlying Zhanganbu Formation (Figure 2(a)). The sediments of the Ganhegou Formation can be subdivided into four units based on the depositional features observed in the XL15-1-01 borehole, as described below.

The lower unit is dominated by a grain-supported conglomerate (facies Gms and Gm) with a lenticular sandstone body or by coarse-grained conglomeratic sandstone (facies Ss). The conglomerates are sub-angular and poorly sorted. Erosive bases and massive bedding are observed in these deposits. The sediments in this section are considered to have formed in an alluvial fan.

The lower–middle unit is dominated by upward-fining cycles of conglomerate (facies Gt and Gm), pebble sandstone, and a thin-bedded mudstone (facies Fm) or siltstone (facies Sm) in the Ganchengzi area (XL15-1-01 borehole). These features were formed by a lateral point-bar accretion or vertical channel aggradation, suggesting the deposition in a braided river environment.

Upsection, in the middle–upper unit of the Ganhegou Formation, the thickness of the conglomerate (facies Gp and GP) decreases, and the thicknesses of the siltstone and mudstone (facies Fl and Fm) increase, suggesting a deposition in a fluvial delta environment. However, these are the only fluvial delta deposits (Figure 6(g,h)) found in the Qingtongxia area and in the eastern Niushou Mountain.

The fine-grained sediments in the upper unit of the Ganhegou Formation are mainly yellow–brown fine sandstone (facies Sr and Fm), argillaceous siltstone, and mudstone (Figure 6(i); facies Mu and Ml) with a horizontal or massive bedding. These sediments were deposited in a lacustrine environment. Above them, the top of the Ganhegou Formation consists of medium- to thick-bedded conglomerate (facies Gms, Gmu, and Gm) with lenticular sandstone (facies Fm) bodies. The clasts are poorly sorted and grain-supported. The erosive surfaces are observed at the bottom of the conglomerate beds. These sediments are interpreted as alluvial fan deposits. In addition, the Ganhegou Formation overlies the Zhanbenbu Formation across a parallel or locally angular unconformity that represents a depositional hiatus of ~0.59 Myr. This hiatus indicates that the area of the Yinchuan Basin was uplifted after the deposition of the Zhanbenbu Formation.

4. Sedimentary facies distribution and palaeocurrents

The Shikouzi Formation is sparsely distributed in the studied area (Figure 7). In the Yinchuan Basin, it is mainly exposed in the Hongdunshan area as coarse clastic alluvial fan sediments in upward-fining sequences coming from the north and northwest in the lowermost and uppermost parts, respectively. In the Helan Mountain, the Shikouzi Formation comprises alluvial fan and fan delta deposits with palaeocurrent directions to the west. On the western margin of the Helan Mountain, the Shikouzi Formation comprises coarse alluvial fan debris with palaeocurrent directions to the southwest. As a whole, the sediments of Shikouzi Formation in studied area were deposited in an alluvial fan or a fan delta in the small catchment basins.

The Qingshuiying Formation is widely distributed in the Yinchuan Basin, with thin conglomerates of an alluvial fan occurring at the bottom grading upward into conglomerates with interbedded sandstone and mudstone of a fan delta. The mudstone-dominated uppermost part represents a stable and long-term lacustrine deposition (Figure 5). The palaeocurrent directions on the eastern and western Yinchuan Basin

and in the western margin of the Helan Mountains are all eastward (Figure 7). This indicates that the terrain was elevated to the west and depressed to the east of the Yinchuan Basin during the Oligocene. The Qingshuiying Formation was directly deposited on the bedrock that formed the Helan Mountain body, and mainly lacustrine mudstones are exposed on both sides of the Helan Mountain (Figures 7(b) and 8 B-B') and in the Niushou Mountain (Figure 7). This evidence indicates that these two mountain ranges formed after the Oligocene. Mudstones with thicknesses of >1000 m (Figure 8C–C') and >150 m (Figure 5(g)) were developed on the western and eastern margins of Niushou Mountain, respectively, indicating that the area of the Niushou Mountain may be one of the sedimentary centres of the Yinchuan Basin during the Oligocene. Furthermore, the data of five boreholes that distributed in different parts of the eastern Yinchuan Basin (Figure 2(a)) indicates that the lacustrine mudstone of the Qingshuiying Formation with a thickness of ~130 m is widely spread in the eastern part of the Yinchuan Basin. It is considered that a unitive lake existed in the area of the Yinchuan Basin and its periphery since the extensive development of the thick layer of mudstone in the upper section of the Qingshuiying Formation in the studied area and adjacent area.

Alluvial fan conglomerates are found in the lower Zhanbenbu Formation on both sides of the Helan Mountains (Figure 7). A thick layer of grey–white marlstone (facies P) interbedded with conglomerate is exposed on the west side (Figures 5(S3) and 9(a)), and thick layers of conglomerates are exposed on the east side (Figure 9(b)), whereas orange–red sandstone and mudstone are found in the Yinchuan Basin. In addition, the palaeocurrent directions change from eastward at the top of the Qingshuiying Formation to westward at the bottom of the Zhanbenbu Formation on the west side of the Helan Mountain. The palaeocurrent directions at the east side of the Helan Mountain are predominantly to the east (Figure 7). This evidence suggests that the uplift of the Helan Mountain began in the early Miocene. The present-day structure of the Yinchuan Basin, with the Helan Mountains uplift as its western boundary, began to form during the early Miocene. Thick mudstones deposited at the eastern periphery (Figures 5(S7) and 7(c)) and in the NW area of the Niushou Mountain (Figures 7(c) and 8C–C'), with thicknesses of >1500 m and >600 m, respectively, indicate that the area of the present-day Niushou Mountain was a sedimentation centre during the Miocene.

The Ganhegou Formation in the Yinchuan Basin is mainly distributed along the east side of the

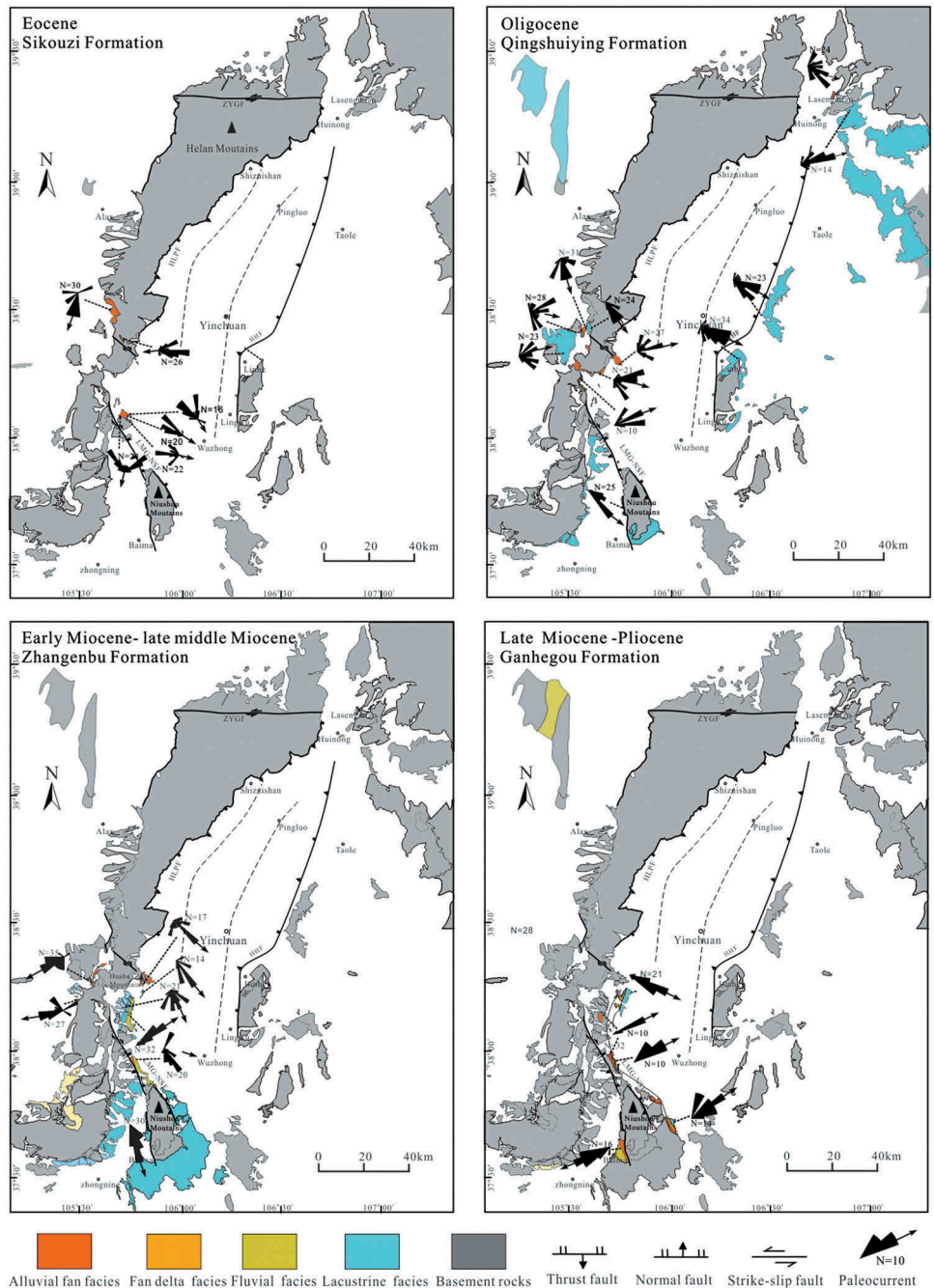


Figure 7. Maps of changing sedimentary facies distribution in the Yinchuan Basin and adjacent areas with time. HLPF – Helan Mountain piedmont fault, HHF – Huanghe (Yellow River) fault, ZYGF – Zhengyiguan fault, LMG-NSF – Liumugao-Niushoushan fault.

Liumugao–Niushoushan Fault (Figure 7). The alluvial fan facies near the fault show a gradual NE transition to fan delta facies and lacustrine facies, indicating that the Liumugao–Niushoushan fault controlled the deposition of the Ganhegou Formation. The palaeocurrent directions are to the northeast on the western margin of the Niushoushan Mountains and to the southwest on the western margin, indicating rapid uplift of the mountains as a result of thrusting upon the Liumugao–Niushoushan fault.

5. Structural deformation and basin tectonic setting

5.1 Eocene–late middle Miocene

The sedimentation in the Yinchuan Basin is closely related to its tectonic setting. The analysis of structure deformation in and around the Yinchuan Basin contributes to the better understanding of the tectonic evolution process of the Yinchuan Basin.

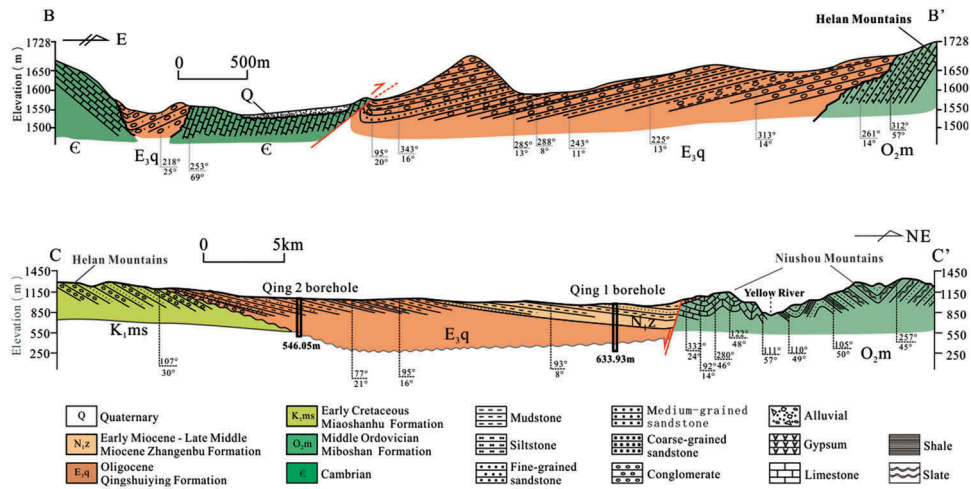


Figure 8. Measured cross-sections along the western part of the Helan Mountains (B–B'; top), and in the southwestern Yinchuan Basin (C–C'; bottom). The locations of the sections are shown in Figure 2a.

There are many faults developed in the Yinchuan Basin and its surrounding areas. These faults are characterized by thrusting in the early stage; however, they became the normal faults after reversing in the direction of movement in the late stage. As it can be seen in the interpreted seismic-reflection profile (Figure 10), the thrust faults cut the strata from the Jurassic to Archean, but their activity ended at beginning of the Cretaceous. This indicates that the thrusting activities of these faults ceased to move at the beginning of the Early Cretaceous. The Late Cretaceous–Palaeocene strata were not deposited in the study area and the adjacent area. It is suggested that the regional uplift happened in the studied area during the period of the Late Cretaceous–Palaeocene and formed the Yinchuan palaeo-uplift. From the Eocene, the topography of the studied area began to decline and to accumulate sediments under the extensional tectonic setting. Therefore, the faults reversion seen in Figure 10 should have occurred in the Eocene. In other words, the Yinchuan palaeo-uplift began to disintegrate during the Eocene, and the Sikouzi Formation was deposited in local depressions.

The stratigraphic changes in facies associations and palaeocurrent directions track the evolving depositional systems during the Eocene. The coarse-grained alluvial fan deposits (FA1, FA2, and FA4 facies associations), coupled with multiple origins for the Sikouzi Formation, indicate that the Eocene basins formed synchronously with the disintegration of the Yinchuan palaeo-uplift. Therefore, the Sikouzi Formation was deposited in an extensional regime. The presence of the Sikouzi Formation from the inner Helan Mountains to the western margin of the Yinchuan Basin indicates

that no obvious geomorphological differentiation occurred in studied area during the Eocene.

The deposition of the Oligocene Qingshuiying Formation in the Yinchuan Basin was controlled by the long-term activity of contemporaneous faults. The growth of strata associated with normal faults is developed in the mudstones of the Qingshuiying Formation in the Yinchuan Basin. A series of normal faults dipping to the southeast controlled the deposition of the lower part of the Formation (Figure 11). However, the normal faults did not cut the upper parts of the Formation, consisting mainly of horizontal mudstone layers. Striations on the upper walls of the faults indicate a down-to-SE sense of movement for these normal faults (Figure 11). Therefore, the Yinchuan Basin was in a rifting stage in a NW–SE extensional tectonic setting during the deposition of the lower part of the Qingshuiying Formation and in a depression stage in a tectonic setting. The tectonic activities were relatively weak during the deposition of the middle and upper parts of the Qingshuiying Formation.

The Zhanbenbu Formation occurred in the early Miocene to late-middle Miocene. Thin sandstone beds with granular gypsum (Figure 6(d)) at the base of the formation conformably overlie deep lacustrine mudstones at the top of the Qingshuiying Formation in the Yinchuan Basin. These field relationships indicate an unchanging sedimentary environment during the deposition of the two formations. Huang *et al.* (2013) and Shi *et al.* (2015) also proposed that the Yinchuan Basin was dominated by a NW–SE extension during the early–late middle Miocene.

5.2 Late Miocene to Pliocene

As discussed in section 4, the deposition of the Ganhegou Formation in the southern Yinchuan Basin was controlled

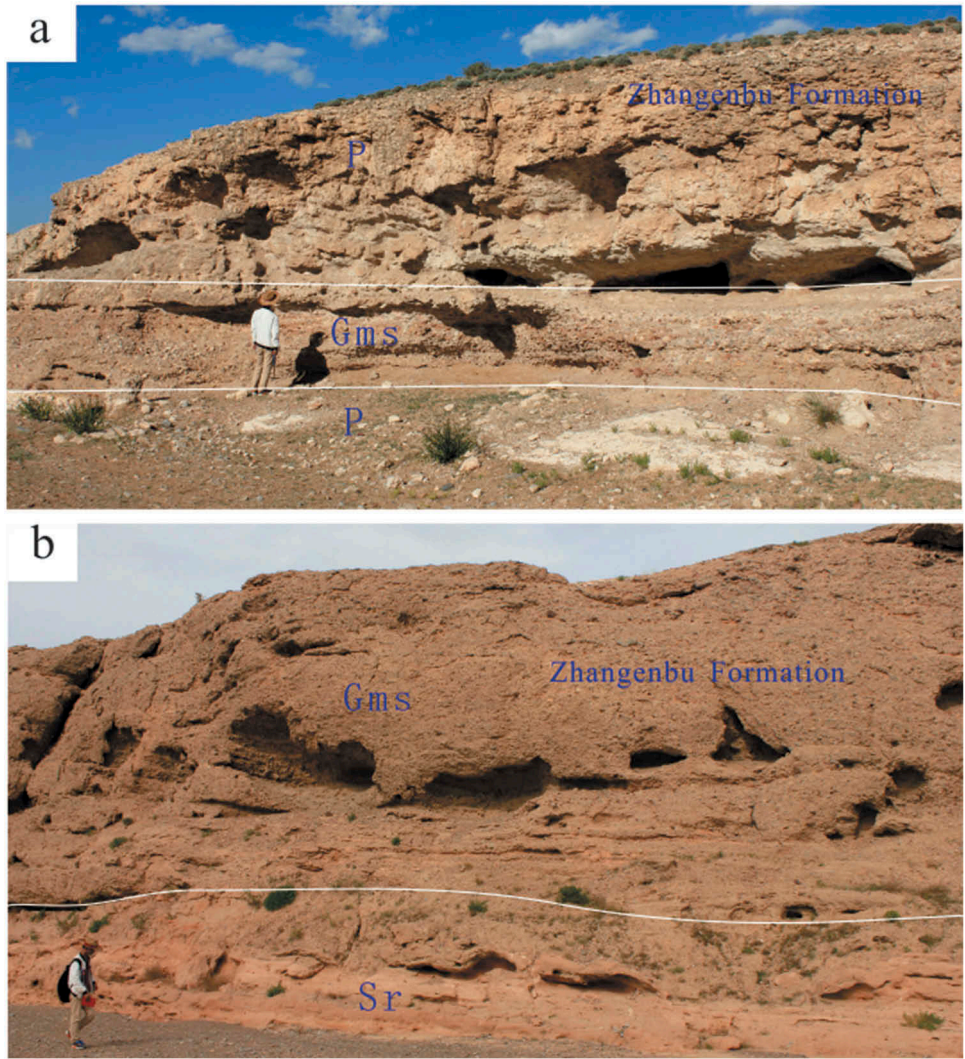


Figure 9. Field photographs of (a) marlstone interbedded with conglomerate in the lower part of the Zhangenbu Formation, western Helan Mountains, (b) conglomerate in the lower part of the Zhangenbu Formation, eastern Helan Mountains. P- Marlstone. Gms – Matrix-supported gravel, Sr – Very fine to coarse-grained sandstone, no grading.

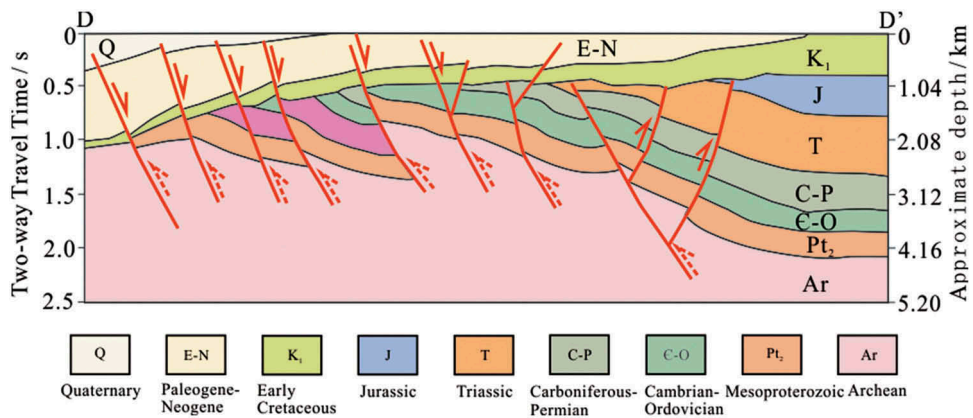


Figure 10. An interpretation from the seismic-reflection profile revealing the structures in and around the Yinchuan Basin (Modified from Hou *et al.* (2014), see Figure 2a for the locations of the profile).

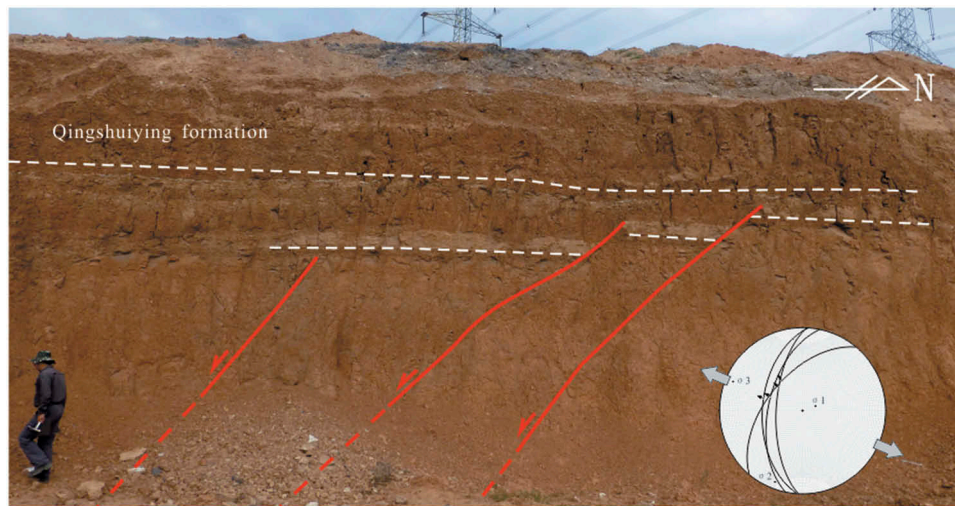


Figure 11. Field photographs of syndimentary structures associated with normal faults in the lower part of the Qingshuiying Formation, eastern Yinchuan Basin (See Figure 2a for the locations of the photo), and the NW-SE extensional stress field based on fault kinematic analysis.

by the Liumugao-Niushou fault. Thus, the activity of the Liumugao-Niushou fault can better reflect the tectonic setting of the basin in late Miocene to the Pliocene.

The Ordovician limestone was thrust on the Early Cretaceous Miaoshanhu Formation as well as on the Miocene Zhangenbu Formation by the Liumugao-Niushou fault (Figure 2(a)). The intersection relationship of the striations in different directions on the fault plane (Figure 12) shows that the early stage of the fault activity was dominated by thrusting, and the latter was dominated by a left-lateral strike-slipping. At the same time, the striations data shows that the fault thrusting was controlled by the NE-SW compression stress. Deep research has been conducted on the activity time of fault (Chen *et al.* 2013; Qin 2018), and the intense activity on the fault began in the late Miocene which was consistent with the initial deposition time of the Ganhegou Formation.

Therefore, the tectonic regime of the Yinchuan Basin was transformed from a dominantly NW-SE extensional setting in the Eocene-late middle Miocene to a dominantly NE-SW compressional setting in the late Miocene. The changes in the tectonic setting caused a brief uplift in the studied area, leading to the Formation of the unconformity between the Ganhegou Formation and the Zhangenbu Formation. The elevation of the landscape was accompanied by the receding of the lake. As a result, the Yinchuan Basin became a denudation area from ~10.17 Ma to ~9.58 Ma. After a short sedimentary discontinuity, the fault depression occurred again in the Yinchuan Basin by the affection of the NW-SE secondary-expansion

resulted from the NE-SW compression. It is suggested that this compression event was in response to the NE expansion of the Tibetan Plateau during the late Miocene-Pliocene which is widely recognized (Lin *et al.* 2010; Wang *et al.* 2011; Shi *et al.* 2013; Wang *et al.* 2013; Zhang *et al.* 2014; Lei 2016). The rapid uplift of the Helan Mountain during the late Miocene (12–10 Ma; Liu *et al.* 2010) may also have resulted from the far field effect of the NE expansion of the Tibetan Plateau.

6. Discussion

6.1 Geodynamic evolution of the Yinchuan Basin

Based on the integration of the data on the Palaeogene-Neogene sedimentary sequence and tectonic structures in the studied area with their respective ages, we propose the following model of the tectonic evolution of the Yinchuan Basin.

6.1.1 Eocene

The Yinchuan Basin is a tectonically controlled basin that formed during the Cenozoic by normal faulting in response to crustal extension. The initial fault-controlled depression of the Yinchuan Basin likely occurred on pre-existing basement thrust faults. The width of the initial basin evolved from the near-parallel to the framing master faults (Illies 1981).

The Yanshan Movement at the end of the Early Cretaceous led to the uplift of the entire studied area and its active erosion until the Cenozoic rift basin formed at the beginning of the Palaeogene (Zhou

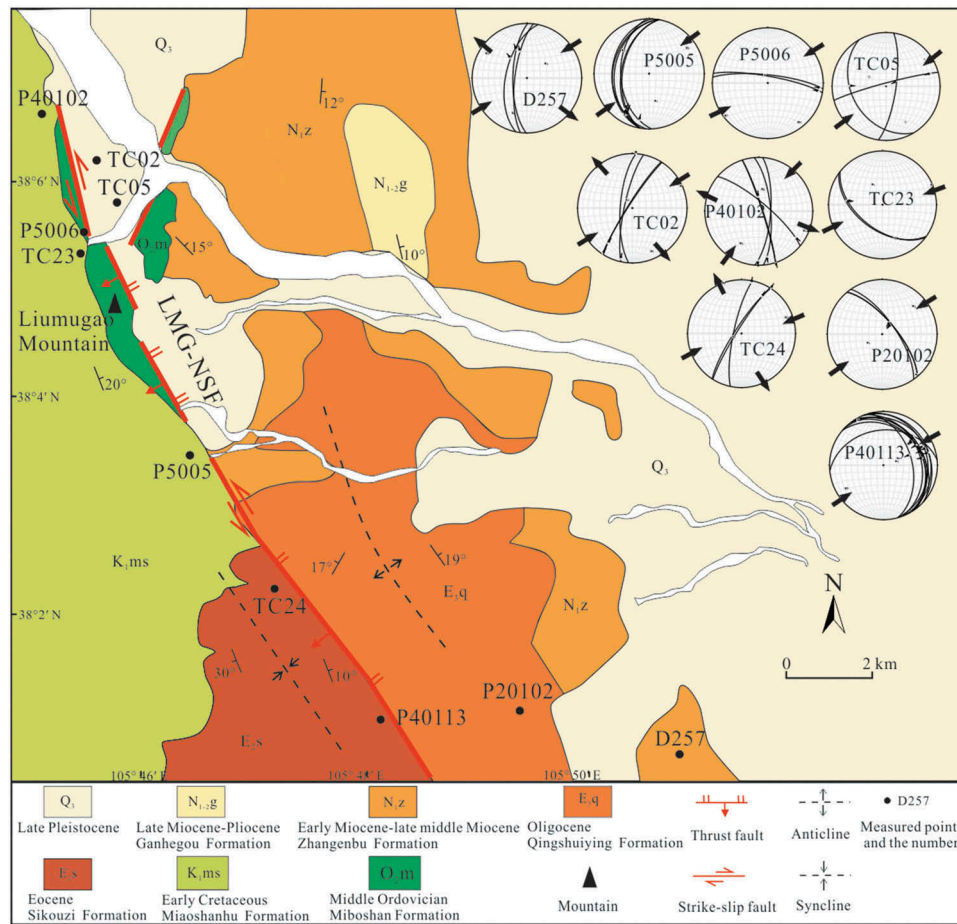


Figure 12. The late Miocene NE–SW Compressive stress showing the deformational features along the LMG-NSF (See Figure 2a for the locations), based on fault kinematic analysis. The opposing arrows show the trends of the maximum principal stress (r_1).

et al. 1985; Wang and Li 2008). During the Eocene, the Yinchuan Basin was mainly filled with alluvial fan–fluvial sediments. The Sikouzi Formation, the earliest sedimentary unit in the basin, is characterized by alluvial fan–fan-delta deposits of small catchment basins during the Eocene (Figure 13(a)).

6.1.2 Oligocene

During the Oligocene, the Yinchuan Basin was in a NW–SE extensional tectonic setting with high topography in the west side and low topography in the east side. The Helan Mountain did not exist at that time, and the lack of unconformities in the studied strata suggests a lack of major tectonic events. Initially, the Yinchuan Basin had a width of ~10 km (NSB 1988; Deng *et al.* 1999), although the western margin of the basin gradually expanded westward during the sedimentation of the Qingshuiying Formation. These observations suggest that the Yinchuan Basin was in a fault depression stage in a NW–SE extensional regime during the deposition of the lower part of the Qingshuiying Formation and in a depression stage in a weakly

extension regime during the deposition of the middle and upper parts of the formation (Figure 13(b)).

6.1.3 Early Miocene to late middle Miocene

During the early–late middle Miocene (21.32–10.17 Ma), the Yinchuan Basin was dominated by a NW–SE extension. The Helan Mountain began to uplift and became the western border of the Yinchuan Basin beginning in the early Miocene (Figure 13(c)) as shown by changes in sedimentary facies and palaeocurrent directions.

6.1.4 Late Miocene to late Pliocene

The NE–SW compression that characterizes the Yinchuan Basin led to distinctive changes in sedimentary facies and sedimentation rates during the late Miocene to Pliocene (Liu *et al.* 2019). The tectonic regime of the basin changed in the late Miocene (~10 Ma), when the NE expansion of the Tibetan Plateau reached the basin. This tectonic event caused a sedimentary discontinuity between the Ganhegou and Zhangebu Formations that represents a hiatus of ~0.59 Myr and increased the sedimentation rates of the

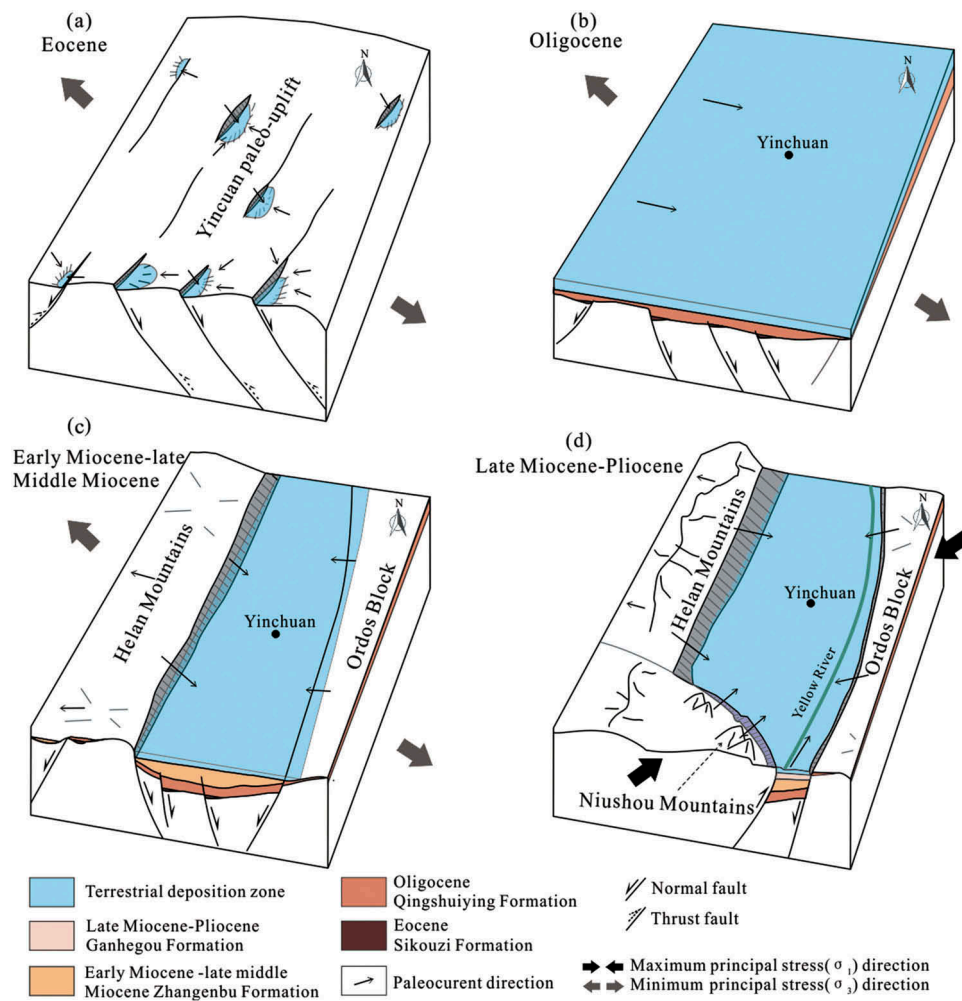


Figure 13. Simplified model of the tectonic evolution of the Yinchuan Basin during the Palaeogene–Neogene.

Ganhegou Formation (Liu *et al.* under review). In addition, the Niushou Mountain in the south began to uplift (Figure 13(d)), and the Helan Mountain in the west experienced a higher rate of uplift (Liu *et al.* 2010). During this period, the Yellow River began to develop and to flow through the Yinchuan Basin from the eastern side of the Niushou Mountain (Chen preparation).

6.2 Dynamic mechanisms

It is generally believed that large-scale interactions among the Pacific, Eurasian, and Indian plates controlled the various styles of rifting and the resultant tectonic evolution in eastern Eurasia (Ren *et al.* 2002; Yin 2010; An *et al.* 2011; Liu *et al.* 2017b). The formation and tectonic evolution of the Yinchuan Basin is also closely related to the regional tectonic setting. The Yinchuan Basin was in the NCC tectonic domain during the Eocene–late Miocene (Zhang *et al.* 1999a), whereas it was mainly influenced by the Tibetan Plateau tectonic domain after the late Miocene.

A change in relative motion between the Pacific and Eurasian plates and subduction of the Pacific plate represented the main controls on the tectonic evolution of the bordering basins in the western Pacific (Robert 2002). The direction and rate of subduction of the Pacific plate have changed several times since the Mesozoic, resulting in spatial and temporal variations in the stress field in eastern Eurasia (Jurdy 1979; Ren *et al.* 2002). The Eocene–Pliocene tectonic evolution of the Yinchuan Basin in the NCC is consistent with far-field effects related to changes in the convergence rates and directions of the Indian–Eurasian and Pacific–Eurasian plate collisions.

The convergence rate between the Pacific and Eurasian plates decreased from 120 to 140 mm/y in the Late Cretaceous to the lowest value of ~30–40 mm/y in the Eocene (Northrup *et al.* 1995). This decrease may have slowed the transmission of horizontal compressive stress between the two plates, leading to large-scale extension near the eastern edge of the Eurasian plate. These processes can also explain the onset of sediment accumulation in the Yinchuan

Basin after the collapse of the Yinchuan palaeo-uplift west of the NCC. The convergence rate gradually increased beginning in the Oligocene. As a result, the research area was still dominated by fault depression in the early Oligocene. The extension slowed, and the Yinchuan Basin gradually evolved into a depression stage during the middle Oligocene. The convergence rates decreased again to 65–70 mm/y during the early–middle Miocene (Northrup *et al.* 1995), which coincides with the NW–SE extension in eastern Asia, including the Yinchuan Basin. During this stage, the Bohaiwan Basin, East China Sea, South China Sea, and other basins were in a post-rift regional subsidence stage, which formed a broad depression (Ren *et al.* 2002). In the Eocene–late Middle Miocene, the Yinchuan Basin was in the post-arc extension environment driven by the subduction of the Pacific plate. The formation and evolution of the Yinchuan Basin may be also affected by deep tectonic–thermal processes: Weak and random anisotropy appeared in the Yinchuan Basin, where the mantle fabric may have been severely disrupted by the most significant lithospheric modification. Flow beneath the pre-existing weak zones driven by the Pacific plate subduction may be responsible for the lithospheric modification processes (Bao *et al.* 2011).

Beginning in the late Miocene (~10 Ma), the tectonic regime in the Yinchuan Basin changed after the NE expansion of the Tibetan Plateau reached the studied area. The tectonic evolution of the basin during this stage is interpreted to reflect the far field effect of the NE expansion of the Tibetan Plateau, driven by the collision between the Indian and Eurasian plates. The distribution direction of Yinchuan Basin is nearly perpendicular to the leading edge fault (LMG-NSF) of the arc-shaped thrust belt in the northeastern margin of the Tibetan Plateau, and the strike-slip faults are developed at the boundary. Therefore, the development of the Yinchuan Basin since the late Miocene is similar to the ‘Impactogen’ model established by Burke (1980).

Conclusions

The conclusions of this study are summarized in the following points.

1. The Palaeogene–Neogene sedimentary sequence of the Yinchuan Basin comprises the Sikouzi, Qingshuiying, Zhangenbu, and Ganhegou Formations from bottom to top. The Sikouzi Formation consists mainly of coarse clastic rocks, and the Qingshuiying Formation consists of mudstones with thin layers of conglomerates at the bottom. Mudstones or gypsum-bearing fine sandstones characterize the lower parts of the Zhangenbu Formation,

with grain sizes showing an upward increase. The lower part of the Ganhegou Formation consists of alluvial–fluvial deposits, whereas the upper part comprises fine clastic deposits.

2. The Yinchuan Basin experienced two major stages of tectonic evolution during the Eocene–Pliocene. During the first stage, a NW–SE extension dominated the deposition from the Eocene to the late middle Miocene. The Helan Mountain was first uplifted during the early Miocene and became the western boundary of the Yinchuan Basin. During the second stage, a NE–SW compression dominated the deposition in the Yinchuan Basin. The Ganhegou Formation was deposited during the late Miocene–Pliocene after a sedimentary hiatus of ~0.59 Ma. The Niushou Mountain began to uplift during the late Miocene and formed the southern boundary of the Yinchuan Basin.

3. Convergence between the Pacific and Eurasian plates controlled the tectonic evolution of the Yinchuan Basin during the Palaeogene–late middle Miocene. Beginning in the late Miocene, the tectonic evolution of the Yinchuan Basin was affected by NE expansion of the Tibetan Plateau, driven by convergence between the Indian and Eurasian plates.

Acknowledgments

The authors thank Xiang Qin and Guodong Bao for assistance in fieldwork. In addition, the authors are very grateful to the editors and anonymous reviewers for offering critical, constructive comments, which helped to improve the manuscript.

Disclosure statement

No potential conflict of interest was reported by the authors.

Funding

This work was supported by the China Geological Survey [DD20160060] and National Science Foundation of China [41672203].

Highlights

- The western and southern boundaries of the Yinchuan basin were formed in the early Miocene and the late Miocene, respectively.
- The Yinchuan Basin was dominated by NW–SE extension in the Eocene–late middle Miocene and dominated by NE–SW compression in the late Miocene.
- The evolution of the Yinchuan basin was influenced by the northeastward expansion of the Tibetan plateau since the late Miocene.

References

- An, M.J., Zhao, Y., Feng, M., Yang, Y.S., Xu, Q.M., Hao, J.J., and Tan, C.X., 2011, What resulted in new tectonic activities in the eastern North China Craton in the Neogene: *Earth Science Frontiers*, v. 18, p. 121–140. [in Chinese with English abstract.]
- An, Z., Kutzbach, J.E., Prell, W.L., and Porter, S.C., 2001, Evolution of Asian monsoons and phased uplift of the Himalayan–Tibetan Plateau since Late Miocene times: *Nature*, v. 411, p. 62–66. doi:10.1038/35075035.
- An, Z.S., Zhang, P.Z., Wang, E.C., Wang, S.M., Qiang, X.K., Li, L., Song, Y.G., Chang, H., Liu, X.D., Zhou, W.J., Liu, W.G., Gao, J. J., Li, X.Q., Shen, J., Liu, Y., and Ai, L., 2006, Changes of the monsoon-arid environment in China and growth of the Tibetan plateau since the Miocene: *Quaternary Sciences*, v. 26, p. 678–692.
- Bao, X.W., Xu, M.J., Wang, L.S., Mi, N., Yu, D.Y., and Li, H., 2011, Lithospheric structure of the Ordos Block and its boundary areas inferred from Rayleigh wave dispersion: *Tectonophysics*, v. 499, p. 132–141. doi:10.1016/j.tecto.2011.01.002.
- Burchfiel, B.C., Zhang, P.Z., Wang, Y.P., Zhang, W.Q., Song, F.M., Deng, Q.D., Peter, M., and Leigh, R., 1991, Geology of the Haiyuan fault zone, Ningxia-Hui autonomous region, China, and its relation to the evolution of the northeastern margin of the Tibetan plateau: *Tectonics*, v. 10, p. 1091–1110. doi:10.1029/90TC02685.
- Burke, K., 1980, Intracontinental rifts and Aulacogens: Geophysics Study Committee, *In Continental Tectonics*: National Academy of Sciences, Washington, p. 42–49.
- Chai, C.Z., Meng, G.K., Du, P., Wang, Y., Liu, B.J., Shen, W.H., Lei, Q.Y., Liao, Y.H., Zhao, C.B., Feng, S.Y., Zhang, X.H., and Xie, X.F., 2007, Comprehensive multi-level exploration of buried active fault: An example of Yinchuan buried active fault: *Seismology and Geology*, v. 21, p. 225–235.
- Chen, F.J., Wang, X.W., Chen, Z.N., and Yang, J., 2004, Analysis of extensional faulted basin: Beijing, Geological Publishing House, p. 10–21. [in Chinese with English summary.]
- Chen, H., Hu, J.M., Gong, W.B., and Li, L.B., 2013, Cenozoic deformation and evolution of the Niushou Shan-Luo Shan fault zone in the northeast margin of the Tibet Plateau: *Earth Science Frontiers*, v. 20, p. 18–35. [in Chinese with English abstract.]
- Deng, J.F., Xiao, Q.H., Qiu, R.Z., Liu, C., Zhao, G.C., Yu, B.S., Zhou, S., Zhong, C.T., and Xu, W.Z., 2006, Cenozoic lithospheric extension and thinning of north China mechanism and process: *Geology in China*, v. 33, p. 751–761. [in Chinese with English abstract.]
- Deng, Q.D., Cheng, S.P., Min, W., Yang, G.Z., and Reng, D.W., 1999, Discussion on Cenozoic Tectonics and dynamics of Ordos block: *Journal of Geomechanics*, v. 5, p. 13–22.
- Fan, G.G., W, L., 2002, Geological condition analysis of ground hot water formation in Yinchuan basin: *Journal of Xi'an Engineering University*, V.24, p. 28-31.
- Fang, S.M., Zhao, C.B., Chai, C.Z., Liu, B.J., Feng, S.Y., Liu, M.J., Lei, Q.Y., and Liu, H., 2009, Seismic evidence of crustal structures in the Yinchuan faulted basin: *Chinese Journal of Geophysics*, v. 52, 1768–1775. [in Chinese with English abstract.] doi:10.1002/cjg2.1435.
- Feng, S.Y., Gao, R., Long, C.X., Fang, S.M., Zhao, C.B., Kou, K.P., Tan, Y.L., and He, H.Y., 2011, The compressive stress field of Yinchuan graben: Deep seismic reflection profile: *Chinese Journal of Geophysics*, v. 54, p. 692–697. [in Chinese with English abstract.]
- Gobo, K., Ghinassi, M., and Nemec, W., 2015, Gilbert-type deltas recording short-term baselevel changes: Delta-brink morphodynamics and related foreset facies: *Sedimentology*, v. 62, p. 1923–1949. doi:10.1111/sed.12212.
- Han, P., Liu, C.Y., Gao, F., Fang, J.J., and Wang, J.Q., 2008, A paleomagnetic study of the Cenozoic Sikouzi Formation in Guyuan, Ningxia: *Journal of Stratigraphy*, v. 32, p. 315–320.
- Hancock, P.L., and Bevan, T.G., 1987, Brittle modes of foreland extension: *Geological Society of London*, v. 28, p. 127–137. doi:10.1144/GSL.SP.1987.028.01.10.
- Harrison, T.M., Copeland, P., Kidd, W.S., and Yin, A., 1992, Raising Tibet: *Science*, v. 255, p. 1663–1670. doi:10.1126/science.255.5052.1663.
- Horton, B.K., and Schmitt, J.G., 1996, *Sedimentology of the lacustrine fan-delta system, Miocene Horse Camp formation, Nevada, USA*: Sedimentology, v. 43, p. 133–155. doi:10.1111/j.1365-3091.1996.tb01464.x.
- Hou, X.B., Yin, K.M., Lin, Z.K., Han, X.Y., and Chen, W., 2014, The study of tectonic inversion, evolution, and superposition of Yinchuan Basin: *Geological Journal of China Universities*, v. 20, p. 277–285. [in Chinese with English abstract.]
- Huang, X.F., Feng, S.Y., Gao, R., and Li, W.H., 2016, Development of the Yinchuan Basin: Deep seismic reflection profile revealed the linkages between shallow geology and deep structures: *Chinese Journal of Geology*, v. 51, p. 53–66. [in Chinese with English abstract.]
- Huang, X.F., Shi, W., Li, H.Q., Chen, L., and Cen, M., 2013, Cenozoic tectonic evolution of the Yinchuan Basin: Constraints from the deformation of its boundary faults: *Earth Science Frontiers*, v. 20, p. 199–210. [in Chinese with English abstract.]
- Illies, J.H., 1981, Mechanism of graben formation: *Tectonophysics*, v. 73, p. 249–266. doi:10.1016/0040-1951(81)90186-4.
- Jurdy, D.M., 1979, Relative plate motions and the formation of marginal basins: *Journal of Geophysical Research*, v. 84, p. 6796–6802. doi:10.1029/JB084iB12p06796.
- Kim, Y.H., Lee, C., and Kim, S.S., 2015, Tectonics and volcanism in East Asia: Insights from geophysical observations: *Journal of Asian Earth Sciences*, v. 113, p. 842–856. doi:10.1016/j.jseaes.2015.07.032.
- Lei, Q.Y., 2016, The extension of the arc tectonic belt in the northeastern margin of the Tibet Plateau and the evolution of the Yinchuan Basin in the western margin of the North China [Ph.D. thesis]: Beijing, China, Institute of Geology, China Earthquake Administration, p. 116–166. [in Chinese with English abstract.]
- Li, J.J., 2013, The uplift of the Qinghai-Tibet Plateau and the environmental changes of the Late Cenozoic: *Journal of Lanzhou University (Natural Sciences)*, v. 49, p. 154–159. [in Chinese with English summary.]
- Li, J.J., Fang, X.M., Song, C.H., Pan, B.T., Ma, Y.Z., and Yan, M.D., 2014, Late Miocene–Quaternary rapid stepwise uplift of the NE Tibetan Plateau and its effects on climatic and environmental changes: *Quaternary Research*, v. 81, p. 400–423. doi:10.1016/j.yqres.2014.01.002.
- Li, J.J., Ma, Z.H., Li, X.M., Peng, T.J., Guo, B.H., Zhang, J., Song, C.H., Liu, J., Hui, Z.C., Yu, H., Ye, X.Y., Liu, S.P., and

- Wang, X.X., 2017, Late Miocene-Pliocene geomorphological evolution of the Xiaoshuizi peneplain in the Maxian Mountains and its tectonic significance for the northeastern Tibetan Plateau: *Geomorphology*, v. 295, p. 393–405. doi:10.1016/j.geomorph.2017.07.024.
- Li, Q.H., Zhang, Y.S., Sheng, G.Y., and Fan, B., 1999, 3D Seismic tomography by using traveltimes and waveform of multi-phase and application to crustal structure in Qilianshan Mt: *CT Theory and Applications*, v. 8, p. 1–9. [in Chinese with English abstract.]
- Li, S.Z., Suo, Y.H., Santosh, M., Dail, M., Liu, X., Yu, S., Zhao, S.J., and Jin, C., 2013, Mesozoic to Cenozoic intracontinental deformation and dynamics of the North China Craton: *Geological Journal*, v. 48, p. 543–560. doi:10.1002/gj.v48.5.
- Lin, A.M., Hu, J.M., and Gong, W.B., 2015, Active normal faulting and the seismogenic fault of the 1739 M_w8.0 Pingluo earthquake in the intracontinental Yinchuan Graben, China: *Journal of Asian Earth Sciences*, v. 114, p. 155–173. doi:10.1016/j.jseaes.2015.04.036.
- Lin, X.B., Chen, H.L., Wyrwoll, K.H., and Cheng, X.G., 2010, Commencing uplift of the Liupan Shan since 9.5 Ma: Evidences from the Sikouzi section at its east side: *Journal of Asian Earth Sciences*, v. 37, p. 350–360. doi:10.1016/j.jseaes.2009.09.005.
- Liu, B.J., Feng, S.Y., Ji, J.F., Wang, S.J., Zhang, J.S., Yuan, H.K., and Yang, G.J., 2017a, Lithospheric structure and faulting characteristics of the Helan Mountains and Yinchuan Basin: Results of deep seismic reflection profiling: *Science China Earth Sciences*, v. 60, 589–601. [in Chinese with English abstract.] doi:10.1007/s11430-016-5069-4.
- Liu, J.H., Zhang, P.Z., and Zheng, D.W., 2010, Pattern and timing of late Cenozoic rapid exhumation and uplift of the Helan Mountain, China: *Earth Sciences*, v. 53, p. 345–355.
- Liu, S.F., Gurnis, M., Ma, P.F., and Zhang, B., 2017b, Reconstruction of northeast Asian deformation integrated with western Pacific plate subduction since 200 Ma: *Earth-Science Reviews*, v. 175, p. 114–142. doi:10.1016/j.earscirev.2017.10.012.
- Liu, S.F., Zhang, J.F., Hong, S.Y., and Ritts, B.D., 2007, Early Mesozoic basin development and its response to thrusting in the Yanshan fold-and-thrust belt, China: *International Geology Review*, v. 49, p. 1025–1049. doi:10.2747/0020-6814.49.11.1025.
- Liu, X.B., Shi, W., Hu, J.M., JFu, J.L., Yan, J.Y., and Sun, L.L., 2019, Magnetostratigraphy and tectonic implications of Paleogene-Neogene Sediments in the Yinchuan Basin, western North China Craton: *Journal of Asian Earth Sciences*, v. 173, p. 61–69. doi:10.1016/j.jseaes.2019.01.016.
- Menzies, M.A., Xu, Y.G., Zhang, H.F., and Fan, W.M., 2007, Integration of geology, geophysics and geochemistry: A key to understanding the North China Craton: *Lithos*, v. 96, p. 1–21. doi:10.1016/j.lithos.2006.09.008.
- Miall, A.D., 1977, A review of the braided-river depositional environment: *Earth Science Reviews*, v. 13, p. 1–62. doi:10.1016/0012-8252(77)90055-1.
- Miall, A.D., 1978, Lithofacies types and vertical profile models in braided river deposits: A summary: *Fluvial Sedimentology*, v. 5, p. 597–604.
- Miall, A.D., 1996, *The geology of fluvial deposits, sedimentary facies, basin analysis, and petroleum geology*: Berlin, Springer, p. 5–130.
- Molnar, P., Boos, W.R., and Battisti, D.S., 2010, Orographic controls on climate and paleoclimate of Asia: Thermal and mechanical roles for the Tibetan Plateau: *Annual Review of Earth and Planetary Sciences*, v. 38, p. 77–102. doi:10.1146/annurev-earth-040809-152456.
- Molnar, P., and Tapponnier, P., 1975, Cenozoic tectonics of Asia: Effects of a continental collision: *Science*, v. 189, p. 419–426. doi:10.1126/science.189.4201.419.
- National Seismological Bureau (NSB), 1988, *Active fault system around Ordos Massif*: Beijing, Seismological Press, p. 1–30. [in Chinese with English summary.]
- Ningxia Bureau of Geology and Mineral Resources, 1990, *Regional geology of Ningxia Hui autonomous region*: Beijing, Geological Publishing House, p. 194–214. [in Chinese with English summary.]
- Ningxia Bureau of Geology and Mineral Resources, 2017, *China regional geology. Regional geology of Ningxia region*: Beijing, Geological Publishing House, p. 294–318. [in Chinese with English summary.]
- Northrup, C., Royden, L., and Burchfiel, B., 1995, Motion of the Pacific plate relative to Eurasia and its potential relation to Cenozoic extension along the eastern margin of Eurasia: *Geology*, v. 23, p. 719–722. doi:10.1130/0091-7613(1995)023<0719:MOTPPR>2.3.CO;2.
- Pan, Y.S., 1999, Formation and uplifting of the Qinghai-Tibet plateau: *Earth Science Frontiers*, v. 6, p. 153–163. [in Chinese with English abstract.]
- Peng, T.J.G., Li, J.J., Song, C.H., Guo, B.H., Liu, J., Zhao, Z.J., and Zhang, J., 2016, An integrated biomarker perspective on Neogene-Quaternary climatic evolution in NE Tibetan Plateau: Implications for the Asian aridification: *Quaternary International*, v. 18, p. 174–182. doi:10.1016/j.quaint.2015.04.020.
- Philippe, P., and Jose, A., 1984, India-Eurasia collisional chronology has implications for crustal shortening and driving mechanism of plates: *Nature*, v. 311, p. 18–22.
- Qi, J.F., and Yang, Q., 2010, Cenozoic structural deformation and dynamic processes of the Bohai Bay basin province, China: *Marine and Petroleum Geology*, v. 27, p. 757–771. doi:10.1016/j.marpetgeo.2009.08.012.
- Qin, X., 2018, *Morphostructure formation and evolution of the LiuMuGao fault zone in the northeastern margin of the Tibet Plateau* [Master's thesis]: Beijing, China, China University of Geosciences, p. 40–43. [in Chinese with English abstract.]
- Qiu, N.S., Xu, W., Zuo, Y.H., and Chang, J., 2015, Meso-Cenozoic thermal regime in the Bohai Bay Basin, eastern North China Craton: *International Geology Reviews*, v. 57, p. 271–289. doi:10.1080/00206814.2014.1002818.
- Quade, J., 1989, Development of Asian monsoon revealed by marked ecological shift during the latest Miocene in northern Pakistan: *Nature*, v. 342, p. 163–165. doi:10.1038/342163a0.
- Ren, J.Y., Tamaki, K.K., Li, S.T., and Zhang, J.X., 2002, Late Mesozoic and Cenozoic rifting and its dynamic setting in Eastern China and adjacent areas: *Tectonophysics*, v. 344, p. 175–205. doi:10.1016/S0040-1951(01)00271-2.
- Robert, H., 2002, Cenozoic geological and plate tectonic evolution of SE Asia and the SW Pacific: Computer-based reconstructions, model and animations: *Journal of Asian Earth Sciences*, v. 20, p. 353–431. doi:10.1016/S1367-9120(01)00069-4.

- Saylor, J.E., Horton, B.K., Nie, J.S., Corredor, J., and Mora, A., 2011, Evaluating foreland basin partitioning in the northern Andes using Cenozoic fill of the Floresta basin, Eastern Cordillera, Colombia: *Basin Research*, v. 23, p. 377–402. doi:10.1111/bre.2011.23.issue-4.
- Shi, W., Dong, S.W., Liu, Y., Hu, J.M., Chen, X.H., and Chen, P., 2015, Cenozoic tectonic evolution of the South Ningxia region, northeastern Tibetan Plateau inferred from new structural investigations and fault kinematic analyses: *Tectonophysics*, v. 649, p. 139–164. doi:10.1016/j.tecto.2015.02.024.
- Shi, W., Liu, Y., Liu, Y., Chen, P., Chen, L., Cen, M., Huang, X.F., and Li, H.Q., 2013, Cenozoic evolution of the Haiyuan fault zone in the northeast margin of the Tibetan Plateau: *Earth Science Frontiers*, v. 20, p. 1–17.
- Song, C.H., 2006, Tectonic uplift and Cenozoic sedimentary evolution in the northern margin of the Tibetan Plateau [Ph.D. thesis]: Lan Zhou, China, Lanzhou University, p. 149–159. [in Chinese with English abstract.]
- Sun, S.Y., 1982, Oligocene spore and pollen assemblages from the Tongxin district of Ningxia: *Journal of the Institute of Geology, Chinese Academy of Geological Sciences*, v. 4, p. 127–138.
- Tapponnier, P., Peltzer, G., Dain, A.Y., Armijo, R., and Cobbold, P., 1982, Propagating extrusion tectonics in Asia: New insights from simple experiments with plasticine: *Geology*, v. 10, p. 611–616. doi:10.1130/0091-7613(1982)10<611:PETIAN>2.0.CO;2.
- Tapponnier, P., Xu, Z.Q., Françoise, R., Meyer, B., Arnaud, N., Wittlinger, G., and Yang, J.S., 2001, Oblique stepwise rise and growth of the Tibet Plateau: *Science*, v. 294, p. 1671–1677. doi:10.1126/science.105978.
- Tian, Z.Y., Han, P., and Xu, K.D., 1992, The Mesozoic–Cenozoic east China rift system: *Tectonophysics*, v. 208, p. 341–363. doi:10.1016/0040-1951(92)90354-9.
- Uyeda, S., and Kanamori, H., 1979, Back arc opening and the mode of subduction: *Journal of Geophysical Research*, v. 84, p. 1049–1061. doi:10.1029/JB084iB03p01049.
- Wang, M.F., and Li, H.Q., 2008, Geological structural evolution characteristics of Yinchuan Basin in Ningxia: *Science and Technology Information*, v. 3, p. 148–149. [in Chinese with English summary.]
- Wang, W.T., Eric, K., Zhang, P.Z., Zheng, D.W., Zhang, G.L., Zhang, H.P., Zheng, W.J., and Chai, C.Z., 2013, Tertiary basin evolution along the northeastern margin of the Tibetan Plateau: Evidence for basin formation during Oligocene transtension: *Geological Society of America Bulletin*, v. 125, p. 377–400. doi:10.1130/B30611.1.
- Wang, W.T., Zhang, P.Z., and Kirby, E., 2011, A revised chronology for Tertiary sedimentation in the Sikouzi basin: Implications for the tectonic evolution of the northeastern corner of the Tibetan Plateau: *Tectonophysics*, v. 505, p. 100–114. doi:10.1016/j.tecto.2011.04.006.
- Wu, F.Y., Lin, J.Q., Simon, A.W., Zhang, O.X., and Yang, J.H., 2005, Nature and significance of the Early Cretaceous giant igneous event in eastern China: *Earth and Planetary Science Letters*, v. 233, p. 103–119. doi:10.1016/j.epsl.2005.02.019.
- Yin, A., 2010, Cenozoic tectonic evolution of Asia: A preliminary synthesis: *Tectonophysics*, v. 488, p. 293–325. doi:10.1016/j.tecto.2009.06.002.
- Yin, A., and Harrison, M., 2000, Geologic evolution of the Himalayan–Tibetan Orogen: *Annual Review of Earth and Planetary Science*, v. 28, p. 211–280. doi:10.1146/annurev.earth.28.1.211.
- Zhang, P.Z., Burchfiel, B.C., Molnar, P., Zhang, W.Q., Jiao, D.C., Deng, Q.D., Wang, Y.P., Leigh, R., and Song, F.M., 1990, Later Cenozoic tectonic evolution of the Ningxia-Hui Autonomous Region, China: *Geological Society of America Bulletin*, v. 102, p. 1484–1498. doi:10.1130/0016-7606(1990)102<1484:LCTEOT>2.3.CO;2.
- Zhang, P.Z., Zhang, H.P., Zheng, W.J., Zheng, D.W., Wang, W.T., and Zhang, Z.Q., 2014, Cenozoic tectonic evolution of continental eastern Asia: *Seismology and Geology*, v. 36, p. 574–585.
- Zhang, Y., Vergely, P., and Mercier, J.L., 1999b, Pliocene–Quaternary faulting pattern and left-slip propagation tectonics in north China: *Episodes*, v. 22, p. 84–88.
- Zhang, Y.Q., Jacques, L.M., and Pierre, V., 1998, Extension in the graben systems around the Ordos (China), and its contribution to the extrusion tectonics of south China with respect to Gobi-Mongolia: *Tectonophysics*, v. 285, p. 41–75. doi:10.1016/S0040-1951(97)00170-4.
- Zhang, Y.Q., Pierre, V., Jacques, L.M., Wang, Y.M., Zhang, Y., and Huang, D.Z., 1999a, Kinematic History and Changes in Tectonic Stress Regime during the Cenozoic along the Qinling and Southern Tanlu Fault Zones: *Acta Geologica Sinica (English Edition)*, v. 73, p. 264–274. doi:10.1111/j.1755-6724.1999.tb00835.x.
- Zhang, Y.Q., Shi, W., Liao, C.Z., and Hu, B., 2006, Fault kinematic analysis and change in Late Mesozoic tectonic stress regimes in the peripheral zones of the Ordos basin, North China: *Acta Geologica Sinica*, v. 12, p. 85–297.
- Zheng, T.Y., Zhao, L., and Zhu, R.X., 2009, New evidence from seismic imaging for subduction during assembly of the North China Craton: *Geology*, v. 37, p. 395–398. doi:10.1130/G25600A.1.
- Zhou, T.X., Wang, L., and Chao, M.Z., 1985, Morphotectonic patterns of Ningxia Hui autonomous region and its formation and evolution: *Acta Geographica Sinica*, v. 40, p. 215–224.